Statistics of branched flow in a weak correlated random potential

Lev Kaplan

Institute for Nuclear Theory, University of Washington, Seattle, Washington 98195

Recent images of electron flow through a two-dimensional electron gas (2DEG) device show branching behavior that is reproduced in numerical simulations of motion in a correlated random potential [3]. We show how such branching naturally arises from caustics in the classical flow and find a simple scaling behavior of the branching under variation of the random potential strength. Analytic results describing the statistical properties of the branching are confirmed by classical and quantum numerical tests.

During the past decade, major advances in the fabrication and study of mesoscopic (or nanoscale) structures have led to the observation of many novel phenomena, and a fruitful interaction has resulted with simultaneous theoretical progress in the areas of random matrix theory, quantum chaos, and disordered systems. Examples of phenomena that have received much attention include universal conductance fluctuations and weak localization in open quantum dots, and the statistics of conductance peak spacings and heights in the Coulomb blockade regime [1].

More recently, scanning probe microscope technology has allowed for the imaging of current flowing in a 2DEG device [2]. After the electron current passes through a narrow quantum point contact (QPC), the flow shows a striking branch-like behavior [3]. The qualitative features of the observed branching pattern are well reproduced in numerical simulations of quantum wave evolution through a correlated random potential, when the rms potential height and the correlation length of the potential are fixed at their experimentally measured values. Perhaps more surprisingly, the same branches are observed in the corresponding classical simulation, indicating that the experimental phenomenon should have a classical explanation. However, the simulations show that the branches *do not* correspond to valleys in the random potential. Instead, it was suggested that branches may arise from caustics in the classical flow.

We emphasize that the problem of wave flow through a correlated random potential is of general interest and not restricted to the mesoscopic context. For example, similar effects of caustics have been discussed recently in the context of long-range sound propagation through the ocean [4]. We also note that the influence of caustics on waves in random media has been studied as far back as 1977 by Berry [5], who analyzed the moments of the intensity distribution. The related problem of the effect of orbit bifurcations on chaotic wave functions is also a research area of continuing interest [6]. Accordingly, our goal here is not only to make contact with one particular experimental observation but also to make progress more generally in exploring this regime of classical and quantum chaotic behavior.

In the present work, we extend the previous qualitative understanding of branching behavior, arriving at analytical results to be compared with numerics and ultimately with experiment. We focus on propagation in a two-dimensional potential, though the methods apply as well to the three-dimensional case (where branches are replaced by caustic surfaces) and to related problems such as light propagation through a medium with varying refractive index. We concentrate throughout on generic patterns and not on rare events that would occur only in a few realizations of the random ensemble.

Our starting point is a Gaussian-distributed random potential $V(x, y)$ with a Gaussian correlation function,

$$\overline{V(\vec{r})} = 0$$
$$\overline{V(\vec{r})V(\vec{r'})} = v_0^2 e^{-|\vec{r}-\vec{r'}|^2/\xi^2} \,. \tag{1}$$

Without loss of generality, we will use units in which the correlation scale $\xi = 1$; similarly the mass and the initial momentum, taken to be in the $x-$direction, are set to unity. To prevent backscattering and localization on a scale of order ξ, we must require the random potential to be weak relative to the initial kinetic energy, $v_0 \ll E_F = 1/2$. In the experiment [3], $v_0/E_F \approx 0.08$, and all our subsequent analytical expressions are computed to leading order in v_0; however, the results turn out to be qualitatively and even in some respects quantitatively valid for $v_0/E_F = 0.3$ and higher. In this approximation, then, the motion is unidirectional: $p_x(t) = p_x(0) \equiv 1$, $x(t) = t$, and

$$dy(t)/dt = p_y(t), \quad dp_y(t)/dt = -\partial V(t,y)/\partial y. \tag{2}$$

In other words, the two-dimensional dynamics reduces to one-dimensional evolution in the transverse dimension y, under the influence of an effectively time-varying random potential [7]. For numerical purposes, the above classical or quantum y-evolution may be discretized on a scale $\Delta t = \Delta x \ll 1$. The initial condition is zero transverse momentum; classically it is the manifold $p_y = 0$ in the $y - p_y$ phase space.

Stretching and folding of this initial manifold under classical evolution in t (or x) produces simple caustics, or folds, where $\delta p_y(t)/\delta y(0) = \infty$ and the classical intensity in position space diverges [8]. By calculating how long it takes for a trajectory to travel a distance of one correlation length in the transverse $y-$direction, we may easily check that this stretching and folding occurs in the classical dynamics on the characteristic time scale

$$t_0 \equiv v_0^{-2/3} \gg 1 \,, \tag{3}$$

i.e., when the potential is weak, a trajectory must pass over many correlation lengths of the potential in the longitudinal (x) direction before caustics arise. In the following, we eliminate the explicit dependence of branching statistics on the random potential strength v_0 by expressing all results in terms of the scaled time t/t_0.

For $t/t_0 > 1$, the transverse stretching factor defined as $s \equiv \delta y(t)/\delta y(0)$ develops a log-normal distribution,

$$\ln P(s) \approx -\frac{(\ln s - \alpha t/t_0)^2}{\beta t/t_0} \,, \tag{4}$$

where the exponent α is a dimensionless Lyapunov exponent, $\overline{\ln s} = \alpha t/t_0$, while β characterizes the inhomogeneity of the stretching, $\overline{(\delta \ln s)^2} = (\beta/2)t/t_0$. The average amount of stretching in the $y-$direction of an infinitesimal piece of the initial manifold grows exponentially with time as

$$\overline{s} = \overline{\delta y(t)/\delta y(0)} \sim e^{(\alpha+\beta/4)t/t_0} \,. \tag{5}$$

Since folds in the classical manifold typically develop when $\delta y \sim \xi = 1$, the number of caustics also grows exponentially with time as

$$N^{\text{caus}} \sim W e^{(\alpha+\beta/4)t/t_0} \,, \tag{6}$$

where W is the length in the $y-$direction of the initial manifold, i.e., the transverse width of the system in units of the correlation length. The scaling (6) has been checked numerically using several values of the random potential strength v_0.

Because the classical density of trajectories diverges at a caustic, we must perform smoothing of intensity on some scale $b \ll 1$ in the transverse $y-$direction in order to obtain a well-defined branch height. In quantum mechanics, such smoothing is of course taken care of automatically by the uncertainty principle, since caustics cannot be resolved when the phase space area enclosed by the fold is below $\hbar$, and thus $b_{\text{eff}} \sim \hbar^{2/3}$ (see below). We also adopt the convention that the initial intensity (classical density of trajectories or quantum wave function density) is normalized to unity.

When a caustic forms at time t_{form} and transverse position y, the classical $b-$smoothed intensity $I_b(t_{\text{form}}, y)$ of the resulting branch scales as

$$I_b \sim b^{-1/2}[s(0, t_{\text{form}})]^{-1} \,, \tag{7}$$

where $s(0, t_{\text{form}})$ is of course the stretching factor between time 0 and time t_{form} of the piece of the manifold in which the fold occurs. Away from caustics the intensity scales simply as $I_b \sim [s(0,t)]^{-1}$. The extra factor of $b^{-1/2}$ in Eq. (7) ensures that for small b (corresponding to the semiclassical or ray limit of the original quantum or wave problem), caustics always dominate the tail of the intensity distribution, as we have confirmed numerically.

Using the typical behavior of the stretching factor s (Eq. (4)), we now immediately see from Eq. (7) that for $\alpha^{-1} < t_{\text{form}}/t_0 < \frac{1}{2}\alpha^{-1}\ln b^{-1}$, every caustic leads to a visible branch, with intensity $I_b \gg 1$. Once a given branch forms, its intensity immediately begins to decay (though at a slower rate) due to further stretching: $I_b(t,y) \sim b^{-1/2}[s(0,t_{\text{form}})]^{-1}[s(t_{\text{form}},t)]^{-1/2}$, eventually vanishing into the background on a logarithmic time scale $t/t_0 \sim \alpha^{-1}\ln b^{-1} \gg 1$. The number of visible branches reaches its peak value of $N^{\text{branch}} \sim Wb^{-1/2}$ at the time scale $t/t_0 \approx \frac{1}{2}\alpha^{-1}\ln b^{-1}$.

At longer times, $t/t_0 > \frac{1}{2}\alpha^{-1}\ln b^{-1}$, it is no longer true that a typical new caustic results in a visible branch, since the resulting smoothed intensity is generally below the level ($I_b \approx 1$) of the random background. Thus, at these longer times branches appear only at caustics that are formed from pieces of the manifold that have experienced anomalously little stretching compared with the average behavior. The number of such visible branches may be easily estimated by first calculating the number of caustics coming from those regions of the manifold that have stretched by no more than some factor $s_0 \ll \exp(\alpha t/t_0)$. This number is given by the product of the manifold fraction that has stretched by less than s_0 and the number of caustics per unit length resulting from that stretching:

$$\ln \frac{N^{\text{caus}}_{s<s_0}}{W} \approx \frac{-(\ln s_0 - \alpha t/t_0)^2}{\beta t/t_0} + \ln s_0 \,. \tag{8}$$

Inserting the maximal stretching factor $s_0 = e^{(const/2)}b^{-1/2}$ that will still allow a newly-formed caustic to produce a visible branch, we obtain for $t/t_0 > \frac{1}{2}\alpha^{-1}\ln b^{-1}$

$$\ln \frac{N^{\text{branch}}}{W} \approx \left(\frac{1}{2} + \frac{\alpha}{\beta}\right)\left(\ln b^{-1} + const\right) - \frac{\alpha^2}{\beta}\frac{t}{t_0} + O\left(\frac{t_0}{t}\right) \,. \tag{9}$$

Thus, after a rapid initial climb, the number of branches falls off exponentially with scaled time t/t_0, at the rate α^2/β. The inherent ambiguity in defining how high a branch must be above the background to be visible can be absorbed into a multiplicative constant in N^{branch} and does not affect the falloff *rate*.

2

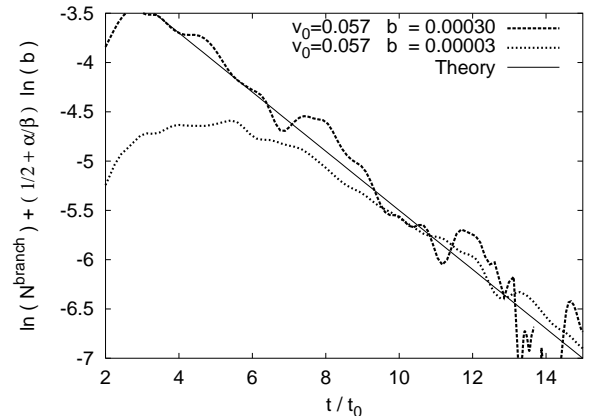FIG. 1. Number of visible branches as a function of dimensionless scaled time t/t_0, where the characteristic time scale t_0 depends on the strength v_0 of the random potential, Eq. (3). A visible branch is defined as an intensity enhancement of at least a factor of 10 above the background. The two dashed curves correspond to different values of the smoothing length b. The solid line represents the predicted exponential falloff at long times (Eq. (9)), with slope $\alpha^2/\beta = 0.30$ ($\alpha = 0.65$, $\beta = 1.42$).

Numerical results are presented in Fig. 1. In this figure and throughout, a single realization of the random ensemble is used for each data curve; no ensemble averaging is necessary to obtain convincing statistics.

In the experimental electron flow images [3], the few longest and most intense branches are the most visually striking. Let us therefore focus on the maximum branch intensity I_b^{max} as a function of scaled time t/t_0. This from Eq. (7) is simply $b^{-1/2}$ divided by the *minimum* stretching factor, which is immediately found by setting $N_{s<s_0}^{\mathrm{caus}} = 1$ in Eq. (8) and solving for $\ln s_0$. We obtain

$$\ln I_b^{\mathrm{max}} \approx \frac{1}{2}\ln b^{-1} - \gamma\frac{t}{t_0}$$
$$\gamma = \alpha - \frac{\beta}{2}\left(\sqrt{1 + \frac{4\alpha}{\beta}} - 1\right) . \qquad (10)$$

This predicted exponential falloff of I_b^{max} with t/t_0 is confirmed in Fig. 2. We note the correct scaling behavior of the maximum intensity for different values of the potential strength v_0 and different smoothing lengths b, as well as good agreement between the theoretically predicted and numerically observed numerical exponent γ. The behavior $I_b^{\mathrm{max}} \sim b^{-1/2}$ confirms that the maximum intensities indeed always come from caustics, which we have also confirmed by direct examination.

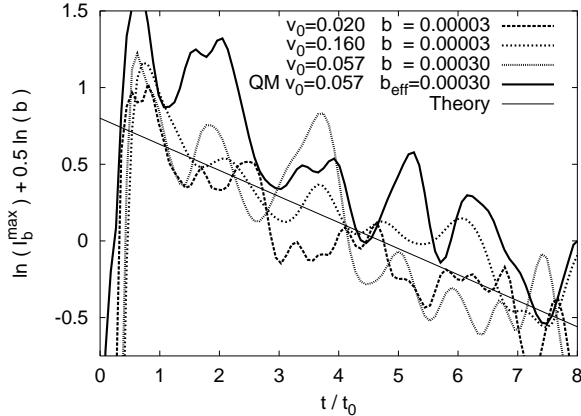FIG. 2. Exponential falloff of maximum branch intensity I_b^{max} with scaled time t/t_0. The three dashed curves correspond to classical simulations for several values of v_0 and smoothing scale b, and the solid curve is a quantum calculation. The power-law dependence of I_b^{max} on b confirms that the peaks arise from simple caustics (folds). Finally, the straight line corresponds to the theoretical prediction of Eq. (10), with analytically predicted exponent $\gamma = 0.17$ ($\alpha = 0.65$, $\beta = 1.42$).

Due to intensity fluctuations within a given branch, particularly in the quantum case, the fraction of space covered by branches, f^{branch}, is in practice a more robust measure than the branch number N^{branch} (Eq. (9)). Defining f^{branch} as the fraction of intensities that exceed some arbitrary cutoff I^{cutoff}, and combining the result of Eq. (10) with the fact that intensity falls off as the inverse square root of the distance as we move away from a caustic, one straightforwardly obtains (for $\beta \geq 2\alpha$)

$$\ln f^{\mathrm{branch}} \approx -2\gamma\frac{t}{t_0} - 2\ln I^{\mathrm{cutoff}} \qquad (11)$$
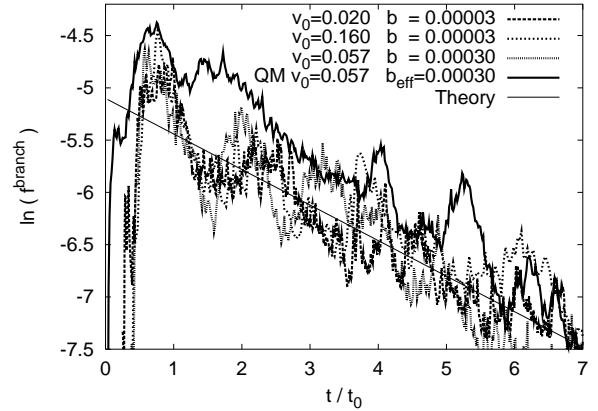

FIG. 3. Fraction of space f^{branch} covered by branches taller than the arbitrary cutoff $I^{\mathrm{cutoff}} = 10$, as a function of scaled time t/t_0. Again, correct scaling is observed under changes of the potential strength v_0. The slope of the solid line is the analytical prediction $2\gamma = 0.34$ of Eq. (11).

Eq. (11) predicts that irrespective of our definition of a branch (i.e., choice of I^{cutoff}), the spatial area covered by visible branches falls off exponentially with distance from the starting point, and the exponent is given by 2γ. This behavior is confirmed in Fig. 3 for several sets of parameters. We note in particular that to leading order the result does not depend on the smoothing scale b, and correspondingly on the ratio of wavelength to correlation length in the quantum or wave problem. Eq. (11) may alternatively be interpreted as giving the cumulative distribution of intensities at a fixed scaled time t/t_0:

$$\int_{I_b}^{\infty} dI_b' \, P(I_b') \sim \exp\left(-2\gamma\frac{t}{t_0}\right) I_b^{-2} , \qquad (12)$$

3

i.e., $P(I_b) \sim I_b^{-3}$. This power-law behavior remains valid until we reach the maximum intensity as given by Eq. (10). The I_b^{-3} falloff means that tall branches do not affect the average intensity, but the mean squared intensity or inverse participation ratio (IPR) is logarithmically divergent in the smoothing scale b. The predicted power-law intensity distribution at fixed time is tested numerically in Fig. 4.
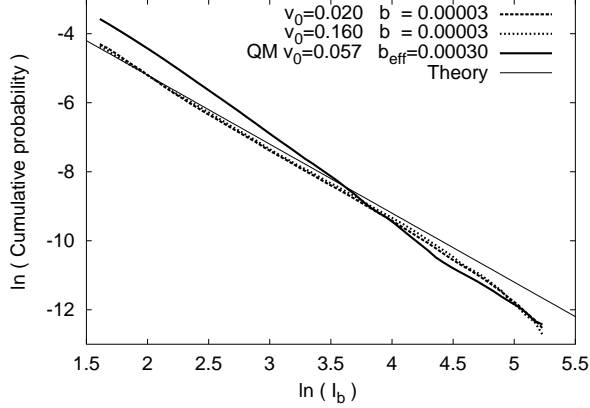

FIG. 4. Cumulative probability distribution $\int_{I_b}^{\infty} dI_b' \, P(I_b')$ of intensities I_b at a fixed scaled time $t/t_0 = 2.2$. The slope -2 of the solid line is the theoretical prediction of Eq. (12). Note that the power-law behavior breaks down as we approach the maximum intensity from Eq. (10), $I_b^{\max} \approx e^{4.5}$ for $b = 0.0003$ and $I_b^{\max} \approx e^{5.5}$ for $b = 0.00003$.

By explicitly tracking all caustic locations for the classical dynamics in Fig. 4, we have also checked that the fraction of large intensities I_b that come from branches associated with caustics ranges from 98.7% for $\ln I_b \geq 2$ to 99.8% for $\ln I_b \geq 4$, while only 3.8% of space overall is covered by such branches at time $t/t_0 = 2.2$. This again provides confirmation that caustics dominate the tail of the intensity distribution.

Our classical results for the branching statistics can be directly applied to the quantum context once we understand the smoothing scale b_{eff} implied by the uncertainty principle in the quantum case. The parabolic structure of the classical manifold near a fold at (y^*, p_y^*) takes the form $y - y^* \sim [(p_y - p_y^*)/p_y^{\text{typ}}]^2$, where p_y^{typ} is the typical value of the transverse momentum, $p_y^{\text{typ}} \sim v_0 t^{1/2} \sim v_0^{2/3}(t/t_0)^{1/2}$. The area enclosed by the fold then scales as $(y - y^*)(p_y - p_y^*) \sim (y - y^*)^{3/2} p_y^{\text{typ}} \sim (y - y^*)^{3/2} v_0^{2/3}$. Setting this area to $\hbar$ and dropping factors of order unity, we finally obtain $y - y^* \sim \hbar^{2/3} v_0^{-4/9}$, i.e., caustics in quantum mechanics do not get resolved below an effective smoothing scale

$$b_{\text{eff}} = \hbar^{2/3} v_0^{-4/9}. \tag{13}$$

We may now simply transcribe our previously obtained classical results, substituting the effective quantum smoothing scale b_{eff} for the explicit classical smoothing scale b. Data from typical quantum calculations appear as solid curves in Figs. 2-4.

In summary, we have made progress towards an analytic and quantitative understanding of branching behavior for flow in a random correlated potential. The key conditions of applicability of these results are (1) a weak random potential $v_0/E_F \ll 1$, (2) a focus on distance scales of order the Lyapunov length, $L_{\text{Lyap}} \sim \xi(v_0/E_F)^{-2/3}$, where ξ is the correlation scale of the potential, and (3) in the quantum case a wavelength no larger than ξ to allow for a simple semiclassical treatment of the caustics. We mention in conclusion that the *numerical values* of the exponents α, β governing the branching statistics may well depend on the details of the random potential, in particular on the precise distribution of potential heights and on the two-point correlation function of the potential (see Eq. (1)). The overall formalism, on the other hand, is more generally applicable provided the log-normal behavior of Eq. (4) is satisfied.

[1] Y. Alhassid, *Rev. Mod. Phys.* **72**, 895 (2000).
[2] M. A. Topinka *et al.*, *Science* **29**, 2323 (2000); M. A. Eriksson *et al.*, *Appl. Phys. Lett.* **69**, 671 (1996).
[3] M. A. Topinka *et al.*, *Nature* **410**, 183 (2001).
[4] M. A. Wolfson and S. Tomsovic, *J. Acoust. Soc. Am.* **109**, 2693 (2001).
[5] M. V. Berry, *J. Phys A* **10**, 2061 (1977).
[6] J. P. Keating and S. D. Prado, *Proc. Roy. Soc. London A* **457**, 1855 (2001).
[7] The approximation is self-consistent because p_y and $p_x - 1$ remain small $(O(v_0^{2/3}))$ over time scales of interest, as we will see below.
[8] Higher-order caustics may also occur, but these have codimension greater than 1 and produce only isolated intensity peaks, not the extended branches that we focus on here.